Preprints, 4th IFAC Conference on
Advances in Proportional-Integral-Derivative Control
Almería, Spain | June 12-14, 2024

Frequency data driven optimal design of different PI control structures for a multivariable process ⋆

Anna Paula V. de A. Aguiar * **Egydio Tadeu G. Ramos** **
George Acioli Júnior * **Péricles R. Barros** *

* *Electrical Engineering Department, Federal University of Campina Grande, Brazil (e-mail: anna.aguiar@ee.ufcg.edu.br, [georgeacioli, prbarros]@dee.ufcg.edu.br).*
** *Post-Graduate Program in Electral Engineering, Electrical Engineering Department, Federal University of Campina Grande, Brazil (e-mail: egydio.ramos@ee.ufcg.edu.br)*

Abstract: Multivariable process are commonly found in industry. The coupling between the different loops makes the control design difficult. In this article, an optimization problem based on the frequency response of the process is used to designed three different multivariable PI control structures. These structures are: centralized control, decentralized control and decentralized controller plus simplified decoupler. To facilitate the centralized control implementation, it is implemented as a decentralized controller plus simplified decoupler. The decoupler is designed using an approximate first-order plus time delay process model. These structures are applied to control a continuous stirred tank reactor with a Van de Vusse chemical reaction, and performance indices are used to compare the obtained results.

Keywords: Process control, multivariable control, PID control.

1. INTRODUCTION

Processes with multiple inputs and multiple outputs (MIMO) are often found in the industry. An example is a chemical reactor, which is an important component to produce highly valuables components (Aguilar-López et al., 2021). These processes have highly nonlinear behavior and interactions/coupling between the different control loops. The closed loop performance is affected by the coupling, because the controller of one loop interferes with the performance of the other loops, which can lead to closed loop instability.

In Vasičkaninová et al. (2016), a comparison between simple and complex fuzzy control and proportional integral derivative (PID) control is presented. The comparison is performed by applying the controllers to the benzene-toluene distillation column, showing that the fuzzy control presented better performance. However, the PI controllers were calculated using the model-based methods Cohen-Coon and Chien-Hrones-Reswick, so modeling errors can affect controller performance. In Gilfred Sam Chandrakumar and Pamela (2021), different control strategies such as PID controller and model predictive control (MPC) are applied to a distillation column. Excellent results are obtained with intelligent controllers combined with model-based control.

Although some articles show better performance of advanced control, the PID controller is most used in practical applications (Nisi et al., 2019). This is because with it is possible to obtain simpler and more efficient control solutions for different industrial applications (Borase et al., 2021). Simple for ease of implementation and maintenance. Effectiveness is related to the good performance achieved in a wide variety of processes.

PI/PID control structures for MIMO processes are classified as: centralized control, decentralized control and decentralized control plus decoupler. Centralized control consists of a full matrix, of which each element is a PI/PID controller. With this structure it is possible to obtain an adequate performance of the closed loop regardless of the coupling degree. A centralized structure disadvantage is that the controller stability is only guaranteed if all the loops are closed. However, in industrial practice, it is common to keep some loops in manual mode due to maintenance (Euzébio et al., 2021).

In decentralized control, the process is divided into single inputs single outputs (SISO) subsystems and SISO control design techniques are used. However, with this structure, closed loop stability or performance requirements may not be achieved. One way to solve this problem is to apply tuning techniques combined with methodologies such as sequential loop closure (Mayne, 1979; Silva Moreira et al., 2021) or use the concept of effective open loop, as presented in Garrido et al. (2021) and Euzébio et al. (2020).

In decentralized control plus decoupler, a block is implemented between the decentralized controller and the MIMO process, in order to reduce the coupling (Aguiar

⋆ This work was supported by Conselho Nacional de Desenvolvimento Científico e Tecnológico (CNPq).

et al., 2020). The decoupled system is treated as multiple SISO loops and less conservative control design methods are applied directly. In general, decoupler design techniques are based on the first-order plus time delay (FOPTD) process model. The decoupler can be static or dynamic. The dynamic is classified as: ideal, simplified or inverted. The simplified decoupler has a simpler structure and is easy to calculate.

In Ahmed (2011) and Yendamuri and Sankar Rao (2019), which addresses decentralized control with and without decoupling of a fluid catalytic cracking unit (FCC) through simulations, it was observed that the control with decoupler was effective, stable and presented better performance in comparison to the control without decoupler. In these articles, controllers are designed based on the identified process model.

A difficulty of the control design for MIMO processes is the process parametric model identification. This task becomes more complicated the greater the process coupling, which can be unfeasible. Thus, techniques based on data in the time or frequency domains have been developed. In Karimi and Kammer (2017), MIMO controller design technique was presented. The technique is based on the multivariable systems frequency response and convex optimization. In Aguiat et al. (2021), constraints of the maximum singular value of the control sensitivity function are added to the problem, in order to guarantee the designed closed loop stability. Process frequency response data and convex optimization are also used in the techniques presented in Boyd et al. (2016).

In this paper, technique presented in Aguiat et al. (2021) is used to design centralized, decentralized PI and decentralized PI control plus simplified decoupler structures. This control structures are applied to pressure and temperature control of a simulated CSTR with a Van de Vusse chemical reaction. The controller is computed solving an optimization problem and without process model knowledge. The simplified decoupler is designed using the model process. Furthermore, a centralized PI controller implementation as a decentralized PI controller plus a simplified decoupler is shown.

This paper is organized as follows. In section 2, the problem statement is presented. The MIMO control design is reviewed in section 3. In section 4, the simulation results are discussed. Finally, the conclusions are in section 5.

2. PROBLEM STATEMENT

Consider a stable linear time invariant multivariable process $\mathbf{G}(s)$ with two inputs and two outputs (TITO), and a PI controller $\mathbf{C}(s)$. The block diagram of the closed loop basic structure is presented in Fig. 1, where $\mathbf{u}(t)$ is the input signals vector (manipulated variables), $\mathbf{y}(t)$ is the output (process variables), $\mathbf{r}(t)$ is the reference, $\mathbf{e}(t)$ is the error and $\mathbf{v}(t)$ is the disturbance.

The TITO PI controller can have a centralized or decentralized structure. In the former, it is represented by:

$$\mathbf{C}_c(s) = \begin{bmatrix} C_{c11}(s) & C_{c12}(s) \\ C_{c21}(s) & C_{c22}(s) \end{bmatrix}, \tag{1}$$

and in the latter:

$$\mathbf{C}_d(s) = \begin{bmatrix} C_{d1}(s) & 0 \\ 0 & C_{d2}(s) \end{bmatrix}. \tag{2}$$

Each non-null element is a PI controller in parallel form:

$$C_{ij}(s) = K_{Pij} + K_{Iij}/s, \tag{3}$$

where K_P and K_I are the proportional and integral gains, respectively.

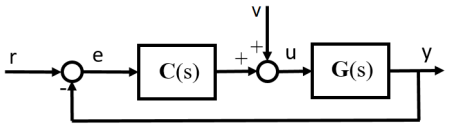

Fig. 1. Closed loop basic structure block diagram.

Considering the closed loop block diagram, Fig. 1, and the loop gain transfer function:

$$\mathbf{L}(s) = \mathbf{G}(s)\mathbf{C}(s), \tag{4}$$

the following sensitivity functions are defined:

- sensitivity:
$$\mathbf{S}(s) = (\mathbf{I} + \mathbf{L}(s))^{-1} \tag{5}$$
- complementary sensitivity:
$$\mathbf{T}(s) = \mathbf{L}(s)(\mathbf{I} + \mathbf{L}(s))^{-1} \tag{6}$$
- control sensitivity:
$$\mathbf{Q}(s) = \mathbf{C}(s)(\mathbf{I} + \mathbf{L}(s))^{-1} \tag{7}$$

The frequency response of the process is given by $\mathbf{G}(j\omega)$. It can be obtained calculated from the process model, by taking $s = j\omega$, or from input ($\mathbf{u}$) and output ($\mathbf{y}$) data points, by applying Fourier transform:

$$\mathbf{G}(j\omega) = \left[\sum_{k=1}^{N-1} y(k)e^{-j\omega T_s k}\right]\left[\sum_{k=1}^{N-1} u(k)e^{-j\omega T_s k}\right]^{-1}, \tag{8}$$

where N is the size of the input/output data vectors, $\mathbf{y}(k)$, $\mathbf{u}(k)$ and $\mathbf{r}(k)$ are the output, the input and the reference signals at instant k, and T_s is the sampling period.

The problem consists in design the PI control for the binary distillation column control such that the closed loop is as close as possible to a given reference model. The centralized, decentralized and decentralized with decoupling control structures will be compared.

The performance indexes used to compare the structures are:

- mean absolute error (MAE):
$$\text{MAE} = \frac{1}{N}\sum_{k=1}^{N} |\mathbf{r}(k) - \mathbf{y}(k)| \tag{9}$$
- mean total value of the control signal (MTV):
$$\text{MTV} = \frac{1}{N}\sum_{k=1}^{N} |\mathbf{u}(k+1) - \mathbf{u}(k)| \tag{10}$$
- mean absolute error with respect to the reference model output (M_r):
$$\text{M}_r = \frac{1}{N}\sum_{k=1}^{N} |\mathbf{y}_d(k) - \mathbf{y}(k)|, \tag{11}$$
which is the error between the designed closed-loop output $\mathbf{y}(k)$ and the reference model output $\mathbf{y}_d(k)$

- rise time (RT): the time it takes for the response to rise from 10% to 90% of the steady-state response
- overshoot (OS): refers to how much the output exceeds the reference signal value.
- robustness: the sensitivity function maximum singular value curve is used to show the designed closed loop robustness. Lower peak values M_S of this curve indicate greater robustness.

3. MIMO PI CONTROLLER DESIGN

In this section, the controller design is presented. An optimization problem is proposed to calculate the PI parameters in order to approximate the closed-loop system by a desired reference model. Constraints in the problem are added in order to ensure closed-loop stability. Then, the method for design the decoupler with inverted structure is presented.

3.1 Controller design

Consider a centralized or decentralized PI controller given by (1) and (2), respectively, and a desired loop gain $\mathbf{L}_d(s)$. For a given controller with parameters θ, the loop gain will be denoted as $\mathbf{L}(s,\theta)$.

The optimization objective is based on Karimi and Kammer (2017), which consists in obtain θ such that the loop gain is closed to the desired in the $\mathcal{H}_\infty$-norm sense, i.e.:

$$\min_{\theta} \ \|\mathbf{L}(s) - \mathbf{L}_d(s)\|_\infty \,, \tag{12}$$

which is equivalent to minimize a scalar $\gamma > 0$, such that:

$$\|\mathbf{L}(s,\theta) - \mathbf{L}_d(s)\|_\infty \leq \gamma, \tag{13}$$

that can be rewritten as:

$$(\mathbf{L}(s,\theta) - \mathbf{L}_d(s))^*(\mathbf{L}(s,\theta) - \mathbf{L}_d(s)) \leq \gamma, \tag{14}$$

where $(\cdot)^*$ is the complex conjugate transpose. Thus, the optimization problem presented is given by:

$$\begin{gathered}\min_{\theta} \gamma \\ \text{subject to:} \\ (\mathbf{G}(s)\mathbf{C}(s,\theta) - \mathbf{L}_d(s))^*(\mathbf{G}(s)\mathbf{C}(s,\theta) - \mathbf{L}_d(s)) \leq \gamma\mathbf{I}.\end{gathered} \tag{15}$$

Applying Schur's complement to (15) leads to:

$$\begin{gathered}\min_{\theta} \gamma \\ \text{subject to:} \\ \begin{bmatrix} \mathbf{I} & (\mathbf{G}(s)\mathbf{C}(s,\theta) - \mathbf{L}_d(s))^* \\ \mathbf{G}(s)\mathbf{C}(s,\theta) - \mathbf{L}_d(s) & \gamma\mathbf{I} \end{bmatrix} \geq \mathbf{0}.\end{gathered} \tag{16}$$

In Aguiat et al. (2021), the constraints on the control sensitivity are inserted into the problem to ensure the closed loop stability. It consists in limiting the peak of the control sensitivity function by a scalar $Q_{max} > 0$: Thus, the optimization problem is given by:

$$\|\mathbf{Q}(s,\theta)\|_\infty \leq Q_{max}. \tag{17}$$

The constraint can be rewritten in the quadratic matrix inequality form:

$$\mathbf{Q}^*(s,\theta)\mathbf{Q}(s,\theta) \leq Q_{max}^2. \tag{18}$$

This constraints is concave-convex. To make the problem convex, first the constraints are rewritten using Schur's complement, and then the concave part is convexified. The linearization of the concave part is performed around a known controller, i.e., the initialization controller $\mathbf{C}_i(s)$.

Thus, the controller gains are computed by solving the following convex optimization problem with LMI constraints Aguiat et al. (2021):

$$\begin{gathered}\min_{\theta} \gamma \\ \text{subject to:} \\ \begin{bmatrix} \mathbf{I} & (\mathbf{G}(s)\mathbf{C}(s,\theta) - \mathbf{L}_d(s))^* \\ \mathbf{G}(s)\mathbf{C}(s,\theta) - \mathbf{L}_d(s) & \gamma\mathbf{I} \end{bmatrix} \geq \mathbf{0} \\ \\ \begin{bmatrix} \Lambda(s,\theta) & (\mathbf{C}(s,\theta)/Q_{max})^* \\ \mathbf{C}(s,\theta)/Q_{max} & \mathbf{I} \end{bmatrix} \geq \mathbf{0},\end{gathered} \tag{19}$$

where:

$$\Lambda(s,\theta) = \mathbf{P}^*(s,\theta)\mathbf{P}_i(s) + \mathbf{P}_i^*(s)\mathbf{P}(s,\theta) - \mathbf{P}_i^*(s)\mathbf{P}_i(s),$$
$$\mathbf{P}(s,\theta) = \mathbf{I} + \mathbf{G}(s)\mathbf{C}(s,\theta), \text{ and } \mathbf{P}_i(s) = \mathbf{I} + \mathbf{G}(s)\mathbf{C}_i(s).$$

The problems (16) and (19) are solved using the frequency response of $\mathbf{G}(s)$. It is not necessary an explicit mathematical model of the process. For that, a large finite set of frequencies is used. The frequency responses can then be obtained by applying (8).

3.2 Simplified decoupler design

The TITO process decoupled with the simplified decoupler is presented in Fig. 2, where the process $\mathbf{G}(s)$ is given by:

$$\mathbf{G}(s) = \begin{bmatrix} G_{11}(s) & G_{12}(s) \\ G_{21}(s) & G_{22}(s) \end{bmatrix}, \tag{20}$$

$\mathbf{u} = \begin{bmatrix} u_1 & u_2 \end{bmatrix}^T$ is the controller output signal vector and $\mathbf{u}' = \begin{bmatrix} u_1' & u_2' \end{bmatrix}^T$ is the input signal vector (manipulated variable). The simplified decoupler $\mathbf{D}(s)$ is the transfer matrix between $\mathbf{u}$ and $\mathbf{u}'$, that is given by:

$$\mathbf{D}(s) = \begin{bmatrix} 1 & D_{12}(s) \\ D_{21}(s) & 1 \end{bmatrix}. \tag{21}$$

It is designed so that the resulting decoupled process:

$$\mathbf{Y}(s) = \begin{bmatrix} G_{11}(s) + G_{12}(s)D_{21}(s) & G_{12}(s) + G_{11}(s)D_{12}(s) \\ G_{21}(s) + G_{22}(s)D_{21}(s) & G_{22}(s) + G_{21}(s)D_{12}(s) \end{bmatrix} \mathbf{U}(s) \tag{22}$$

is diagonal dominant.

Considering the approximate FOPTD model for the process:

$$\hat{\mathbf{G}}(s) = \begin{bmatrix} \dfrac{K_{11}}{\tau_{11}s+1}e^{-sL_{11}} & \dfrac{K_{12}}{\tau_{12}s+1}e^{-sL_{12}} \\ \dfrac{K_{21}}{\tau_{21}s+1}e^{-sL_{21}} & \dfrac{K_{22}}{\tau_{22}s+1}e^{-sL_{22}} \end{bmatrix}, \tag{23}$$

where K_{ij}, τ_{ij} and L_{ij} are the gain, the time constant and the delay of the $G_{ij}(s)$, respectively. Then, the decoupler terms are given by:

$$D_{12}(s) = -\frac{\hat{G}_{12}(s)}{\hat{G}_{11}(s)} = -\frac{K_{12}(\tau_{11}s+1)}{K_{11}(\tau_{12}s+1)}e^{-\eta\tau_{d12}s}, \tag{24}$$

$$D_{21}(s) = -\frac{\hat{G}_{21}(s)}{\hat{G}_{22}(s)} = -\frac{K_{21}(\tau_{22}s+1)}{K_{22}(\tau_{21}s+1)}e^{-\eta\tau_{d21}s}, \tag{25}$$

where $\tau_{d12} = L_{12} - L_{11}$, $\tau_{d21} = L_{21} - L_{22}$ and:

$$\eta(L) = \begin{cases} 1; \text{ if } \tau_{dij} \geq 0 \\ 0; \text{ if } \tau_{dij} < 0, \end{cases}$$

in order to assure that the decoupler is causal.

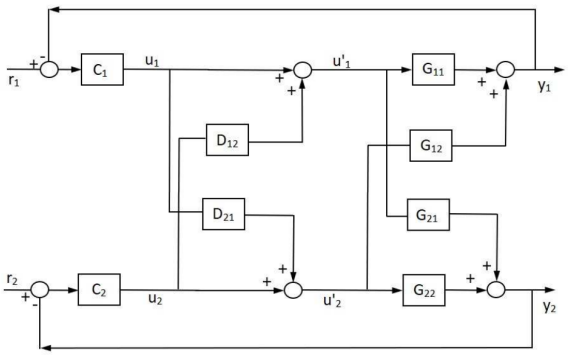

Fig. 2. TITO system with inverted decoupler.

3.3 Centralized controller implementation

The practical implementation and maintenance of the centralized controller is not trivial. To simplify these tasks the centralized controller can be implemented as the decentralized controller plus decoupler.

Considering the TITO process and the decoupler structure, the centralized PI controller $\mathbf{C}_c(s)$ can be rewritten as a product of the decentralized PI controller $\mathbf{C}_d(s)$ and the decoupler $\mathbf{D}(s)$.

$$\mathbf{C}_c(s) = \mathbf{D}(s)\mathbf{C}_d(s) \tag{26}$$

$$\begin{bmatrix} C_{c11}(s) & C_{c12}(s) \\ C_{c21}(s) & C_{c22}(s) \end{bmatrix} = \begin{bmatrix} C_{d1}(s) & C_{d2}(s)D_{12}(s) \\ C_{d1}(s)D_{21}(s) & C_{d2}(s) \end{bmatrix} \tag{27}$$

Thus, the decentralized controller terms are given by:

$$C_{d1}(s) = C_{c11}(s),\ C_{d2}(s) = C_{c22}(s) \tag{28}$$

and the decoupler terms:

$$C_{c12}(s) = C_{d2}(s)D_{12}(s), \tag{29}$$

$$D_{12(s)} = C_{c12}(s)/C_{d2}(s) \Rightarrow D_{12}(s) = C_{c12}(s)/C_{c22}(s). \tag{30}$$

Similarly, $D_{21}(s)$ is given by:

$$D_{21}(s) = C_{c21}(s)/C_{d1}(s) \Rightarrow D_{21}(s) = C_{c21}(s)/C_{c11}(s). \tag{31}$$

4. SIMULATION RESULTS

In this section, the multivariable PI controller structures presented are applied to control a CSTR with a Van de Vusse reaction:

$$\begin{matrix} \mathrm{A} \xrightarrow{k_1} \mathrm{B} \xrightarrow{k_2} \mathrm{C} \\ 2\ \mathrm{A} \xrightarrow{k_3} \mathrm{D} \end{matrix}. \tag{32}$$

This reaction occurs on a vessel, which is fed with compound A and has its temperature is controlled by a cooling jacket. The dynamic model of this process is presented in Aguilar-López et al. (2021). It has highly nonlinear, and can present non-minimal phase or changes in gain signal depending of the operating point.

The control objective is to improve the concentration of compound B. The manipulated variables are the input flow of compound A and the cooling jacket temperature. The process variables are the concentration of B and the reactor temperature.

The process model is simulated using Simulink, and the optimization problems to determine the controllers are solved using CVX framework.

Initially, the FOPTD process model was identified from process open loop step response:

$$\mathbf{G}(s) = \begin{bmatrix} \dfrac{0.08e^{-0.29s}}{0.89s+1} & \dfrac{-0.01e^{-0.42s}}{1.08s+1} \\ \dfrac{-1.70e^{-0.11s}}{0.37s+1} & \dfrac{0.42e^{-0.09s}}{0.65s+1} \end{bmatrix}. \tag{33}$$

By doing a RGA analysis, the best input-output pairing is the input flow and concentration for loop 1, and the cooling jacket temperature and the reactor temperature for loop 2.

The desired loop gain function ($\mathbf{L}_d(j\omega)$) was defined from the closed loop function ($\mathbf{T}_d(j\omega)$):

$$\mathbf{L}_d(j\omega) = \mathbf{T}_d(j\omega)(\mathbf{I} - \mathbf{T}_d(j\omega))^{-1}. \tag{34}$$

The reference model considered is given by:

$$\mathbf{T}_d(s) = \begin{bmatrix} \dfrac{e^{-0.29s}}{0.79s+1} & 0 \\ 0 & \dfrac{e^{-0.09s}}{0.49s+1} \end{bmatrix}. \tag{35}$$

The time constant for the jth loop is $\tau_j = 2(T_{jj} + L_{jj})/3$, where T_{jj} and L_{jj} are, respectively, the time constant and delay of the element $G_{jj}(s)$ in (33) (Aguiar et al., 2023). This was chosen in order to achieve a fast closed loop response. The initialization controller is given by:

$$\mathbf{C}_i(s) = \begin{bmatrix} \dfrac{0.235}{s} & \dfrac{0.005}{s} \\ \dfrac{0.932}{s} & \dfrac{0.044}{s} \end{bmatrix}. \tag{36}$$

In addition, $Q_{max} = 962.89$ was used. The methods for choose this parameters are presented in Aguiar et al. (2023).

To get the process frequency response, the open loop process was excited with a pseudo random binary signal (PRBS) signal. The PRBS response is presented in Fig. 3. The PRBS signal clock period T_{ck} is defined as a function of the estimated dominant process time constant T_{st} (Isermann and Münchhof, 2011):

$$T_{ck} = \frac{T_{st}}{5}. \tag{37}$$

Then, the Fourier transform (8) of the collected input and output signals was performed.

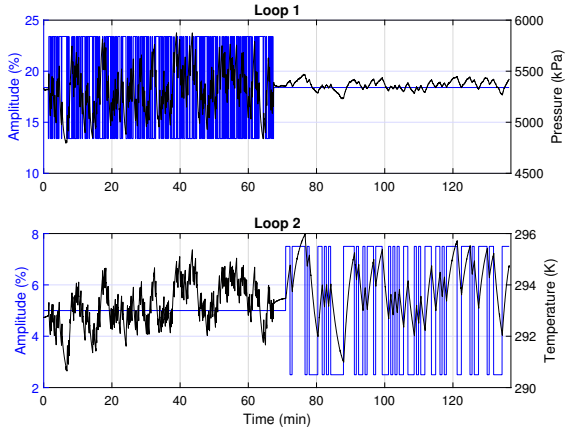

Fig. 3. PRBS open loop experiment

4.1 Controller design

Centralized control Considering the initialization controller (36) and the reference model (35), the centralized controller was designed solving the optimization problem (19). It can be written as a decentralized PI controller plus simplified decoupler, as shown in (27), which results in:

$$\mathbf{C}_1(s) = \begin{bmatrix} 7.94 + \dfrac{21.59}{s} & 0 \\ 0 & 4.79 + \dfrac{7.56}{s} \end{bmatrix}, \tag{38}$$

$$\mathbf{D}_1(s) = \begin{bmatrix} 1 & 0.12\dfrac{0.36s+1}{0.63s+1} \\ 0.25\dfrac{0.37s+1}{0.62s+1} & 1 \end{bmatrix}. \tag{39}$$

Decentralized control plus simplified decoupler The simplified decoupler was designed using (24) and (25). The FOPTD parameters are given by the model in (33). The obtained decoupler transfer matrix was:

$$\mathbf{D}_2(s) = \begin{bmatrix} 1 & 3.98\dfrac{0.65s+1}{0.37s+1}e^{-0.018s} \\ 0.12\dfrac{0.90s+1}{1.08s+1}e^{-0.131s} & 1 \end{bmatrix}. \tag{40}$$

Then, considering the decoupled process (22), the initialization controller (36) and the reference model (35), the decentralized controller was designed solving the optimization problem. The resulting PI controller is given by:

$$\mathbf{C}_2(s) = \begin{bmatrix} 23.17 + \dfrac{21.62}{s} & 0 \\ 0 & 3.98 + \dfrac{7.59}{s} \end{bmatrix}. \tag{41}$$

Decentralized control Considering the diagonal elements of the initialization controller (36) and the reference model (35). The decentralized controller was designed solving the optimization problem (19), by constrained the solution set for $\mathbf{K}_P$ and $\mathbf{K}_I$ to be diagonal. The obtained controller is given by:

$$\mathbf{C}_3(s) = \begin{bmatrix} 11.05 + \dfrac{11.36}{s} & 0 \\ 0 & 2.63 + \dfrac{3.98}{s} \end{bmatrix}. \tag{42}$$

4.2 Results

The three control structures were applied to the concentration and temperature control of the CSTR. At time $t = 0$, a step was applied to the setpoint of the loop 1, with amplitude of 0.2 mol/L. When $t = 10$ min, other step was applied to the setpoint of the loop 2, with amplitude of -10 ^{o}C

In Figs 4 and 5, closed loop step responses and the control signals are presented, respectively. The process outputs with the centralized and decoupler structures led to similar results for setpoint traking and reference output error. When the temperature setpoint was changed, the decoupler had a poor performance in mitigate the disturbance in the concentration. This was due the uncertainties of the FOPTD model used in the design of the decoupler.

The decentralized controller structure led to poor performance both in setpoint tracking for the concentration, as well as in reduce the coupling between the loops.

The performance indices are presented in the table 1. The frequency indexes M_S and $\|\mathbf{Q}(s)\|_\infty$ gives information about robustness of the closed loop and the fullfilment of the constraint Q_{max}, respectively. The time indexes were obtained for each loop using Eqns. (9)-(11).

The decentralized structure have better robustness indexes, but fail to meet the performance requirements. The closed loop system with decoupler controller has good performance results, at cost of a high total variation of the control signals, as can be observed by the MTV indexes and Fig. 5. That said, the centralized controller is the best choice for this scenario, because good results in performance and robustness were achieved.

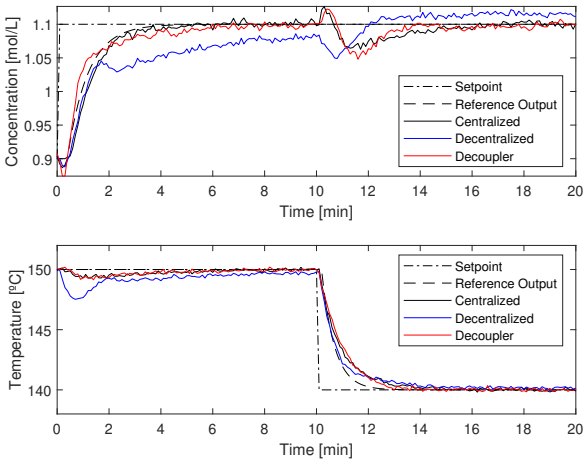

Fig. 4. Closed loop step response

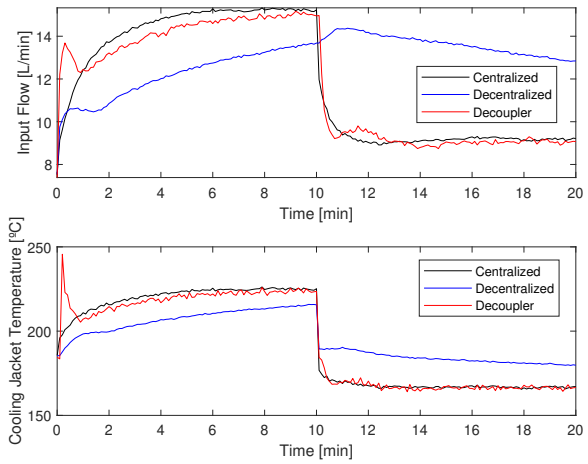

Fig. 5. Control signals

5. CONCLUSIONS

The comparative analysis between three PI MIMO control structures was presented in this article. This structures are centralized control, decentralized control and decentralized

Table 1. Performance indices

	Centralized	Decoupler	Decentralized
M_S	1.58	1.31	14.77
$\|\mathbf{Q}(s)\|_\infty$	146.55	186.66	96.26
	Loop 1		
MAE	0.019	0.018	0.035
MTV	0.097	0.141	0.057
M_r	0.008	0.009	0.023
RiseTime (min)	1.7	2.4	8.6
	Loop 2		
MAE	0.593	0.586	0.835
MTV	0.925	2.01	0.467
M_r	0.290	0.287	0.545
RiseTime (min)	1.1	0.9	1.0

plus simplified decoupler. To design the PI controllers, a design technique based on the process frequency response and formulated as a convex optimization problem was used. The decoupler was designed from the FOPTD process model.

Centralized control resulted in reduced coupling, however the coupling still affects performance. This structure disadvantage is that it is not usually implemented in practice, due to maintenance difficulties. Thus, a way to implement this controller as the decentralized controller plus a simplified decoupler was presented. For a PI structure, the decoupler terms have a lead-lag form.

With the decentralized plus simplified decoupler structure, good performance but poor robustness was obtained, with a high control signal variation. The purely decentralized structure performance was degraded due to the coupling non-cancellation between the loops. Although it is easy to implement in the control system, for the considered process, the closed loop high coupling interferes with the proper functioning.

Thus, it can be concluded that the best performance was obtained when the centralized controller was used. The disadvantage in implementation can be treated by using the decentralized plus simplified decoupler structure. In the simulation study, both results in performance and robustness were obtained for this structure.

REFERENCES

Aguiar, A.P.V.d.A., Acioli Junior, G., and Barros, P.R. (2020). Evaluation and redesign of the inverted decoupler: Open and closed-loop approaches. *International Journal of Control, Automation and Systems*, 18(6), 1435–1444. doi:10.1007/s12555-019-0371-3.

Aguiar, A.P.V.d.A., Acioli Junior, G., and Rezende, B.P. (2023). Frequency-based multivariable control design with stability margin constraints: A linear matrix inequality approach. *Journal of Process Control*, 132, 103–115. doi:10.1016/j.jprocont.2023.103115.

Aguiat, A.P.V.d.A., Acioli Junior, G., Barros, P.R., and Perkusich, A. (2021). A data-driven approach to mimo pid tuning via lmi constraints. *IFAC-PapersOnLine*, 54(20), 573–578. doi:10.1016/j.ifacol.2021.11.233. Modeling, Estimation and Control Conference MECC 2021.

Aguilar-López, R., Mata-Machuca, J.L., and Godinez-Cantillo, V. (2021). A tito control strategy to increase productivity in uncertain exothermic continuous chemical reactors. *Processes*, 9(5). doi:10.3390/pr9050873.

Ahmed, D. (2011). Decoupling control of fluid catalytic cracking unit. *Journal of chemistry and chemical engineering*, 5, 12–19.

Borase, R.P., Maghade, D.K., Sondkar, S.Y., and Pawar, S.N. (2021). A review of pid control, tuning methods and applications. *International Journal of Dynamics and Control*, 9(2), 818–827. doi:10.1007/s40435-020-00665-4.

Boyd, S., Hast, M., and Åström, K. (2016). Mimo pid tuning via iterated lmi restriction. *International Journal of Robust and Nonlinear Control*, 26, 1718–1731. doi:10.1002/rnc.3376.

Euzébio, T., da Silva, M., and Yamashita, A. (2021). Decentralized pid controller tuning based on nonlinear optimization to minimize the disturbance effects in coupled loops. *IEEE Access*, PP, 1–1. doi:10.1109/ACCESS.2021.3127795.

Euzébio, T.A., Yamashita, A.S., Pinto, T.V., and Barros, P.R. (2020). Siso approaches for linear programming based methods for tuning decentralized pid controllers. *Journal of Process Control*, 94, 75–96. doi:10.1016/j.jprocont.2020.08.004.

Garrido, J., Ruz, M.L., Morilla, F., and Vázquez, F. (2021). Iterative method for tuning multiloop pid controllers based on single loop robustness specifications in the frequency domain. *Processes*, 9(1). doi:10.3390/pr9010140.

Gilfred Sam Chandrakumar, A. and Pamela, D. (2021). Withdrawn: Advancements in hybrid controllers and new era models of distillation column: A review. *Materials Today: Proceedings*. doi:10.1016/j.matpr.2020.11.725.

Isermann, R. and Münchhof, M. (2011). *Identification of Dynamic Systems: An Introduction with Applications*. Advanced Textbooks in Control and Signal Processing. Springe Berlin, Heidelberg, 1 edition. doi:10.1007/978-3-540-78879-9.

Karimi, A. and Kammer, C. (2017). A data-driven approach to robust control of multivariable systems by convex optimization. *Automatica*, 85, 227–233. doi:10.1016/j.automatica.2017.07.063.

Mayne, D. (1979). Sequential design of linear multivariable systems. *Proceedings of the Institution of Electrical Engineers*, 126, 568–572(4). doi:10.1049/piee.1979.0135.

Nisi, K., Nagaraj, B., and Agalya, A. (2019). Tuning of a pid controller using evolutionary multi objective optimization methodologies and application to the pulp and paper industry. *International Journal of Machine Learning and Cybernetics*, 10. doi:10.1007/s13042-018-0831-8.

Silva Moreira, L.J., Aguiar, A.P.V.A., Barros, P.R., and Acioli Júnior, G. (2021). Data-driven pid closed-loop evaluation and retuning time and frequency domain approaches. *Journal of Control, Automation and Electrical Systems*, 32(1), 82–95. doi:10.1007/s40313-020-00654-0.

Vasičkaninová, A., Bakosova, M., and Mészáros, A. (2016). *Fuzzy Control of a Distillation Column*, volume 38, 1299–1304. doi:10.1016/B978-0-444-63428-3.50221-6.

Yendamuri, P. and Sankar Rao, C. (2019). Design of robust pi controller with decoupler for a fluid catalytic cracking unit. *Industrial Engineering Chemistry Research*, 58, 20722–20733. doi:10.1021/acs.iecr.9b04770.